Vietnam Journal of Mechanics, Vol. 44, No. 4 (2022), pp. 445 – 458
DOI: https://doi.org/10.15625/0866-7136/17936

VIBROACOUSTIC BEHAVIOR OF A RECTANGULAR COMPOSITE PLATE IN THERMAL ENVIRONMENT

Tran Ich Thinh[1,*], **Pham Ngoc Thanh**[2]
[1]*Hanoi University of Science and Technology, Hanoi, Vietnam*
[2]*Viet Tri University of Industry, Phu Tho, Vietnam*
[*]E-mail: thinh.tranich@hust.edu.vn

Received: 06 December 2022 / Published online: 30 December 2022

Abstract. This paper is a study of the vibroacoustic behavior of orthotropic laminated composite rectangular plate under a sound wave excitation in thermal environments. An improved analytical procedure has been developed that allows for an efficient solution of the finite composite plate sound transmission problem. A symmetrically orthotropic laminated composite plate is considered. The plate is modeled with classic thin-plate theory and is assumed to be clamped on all four sides. The incident acoustic pressure is modeled as a harmonic plane wave impinging on the plate at an arbitrary angle. The sound transmission loss is calculated from the ratio of incident to transmitted acoustic powers.

Keywords: vibroacoustic behavior, laminated composite plate, sound transmission loss, thermal loads.

1. INTRODUCTION

Composite sandwich structures are extensively applied in automotive, marine, and aircraft because of superior stiffness-to-weight ratios. These structures are invariably exposed to the thermal and noise environment in their service life, especially as a component of the hypersonic aircraft

From the 50s up to now, the research problem of the behavior of acoustic vibration through sheet structures (metallic, composite, ...) has received a lot of attention from scientists around the world through various studies, for example. Ko [1] proposed a theoretical model to evaluate noise reduction through an isotropic, infinite iron plate structure using elastic baffles in water and air environments. The study used the transmission matrix method and Fourier series expansion to calculate the sound propagation loss of the structure. Tadue et al. [2, 3] calculated sound transmission loss through infinite single and double steel walls in air and water environments excited by harmonized sound waves. Using the Kirchhoff or Mindlin theory combined with the inverse Fourie function to calculate the sound insulation capacity of environment including isotropic layers, air

and water, were analyzed. Kuo et al. [4,5] studied the sound transmission loss through an infinite orthotropic composite laminated at different frequencies used to transmission matrix method determined by stress and velocity on 2D and 3D models. The experimental and numerically calculated sound transmission loss results were compared, and their material and sound propagation properties were studied and discussed. Thinh and Thanh [6] investigated the vibroacoustic of a clamped finite orthotropic laminated double composite plate with a closed air cavity. Using the method of modal decomposition, a double Fourier series solution is obtained to characterize the vibroacoustic performance of the structure. The sound transmission loss (STL) is calculated from the ratio of incident to transmitted acoustic powers. The accuracy of the solution is shown by comparing the STL values obtained from this presented model with the experimental and theoretical results available in the literature

However, these theoretical and numerical methods could provide direction for engineering design in room temperature. The current there are few literatures about the STL of composite panels in the thermal environment. Meanwhile lots of machineries work in high temperature environment especially aerospace structures. Some of the studies below partly say that, such as, hypersonic aircraft are always exposed to the thermal environment for aerodynamic heating [7,8]. The closed system will introduce thermal stress in the high-temperature environment, which changes the dynamic characteristics of the system significantly. Therefore, investigating composite panels in a thermal environment is of significance. Hoang [9] investigated the nonlinear response of doubly curved functionally graded material sandwich panels resting on elastic foundations in a thermal environment. Frostig [10] presented the classical and high-order computational models of unidirectional sandwich panels with incompressible and compressible cores. Sun et al. [11] carried out compression tests to investigate the mechanical properties of carbon fiber sandwich with the combined core. Wang et al. [12] conducted comprehensive experiments of tandem hexagonal honeycomb structures subjected to axial compression. Caliskan and Apalak [13] addressed the low-velocity impact bending response of sandwich beams with expanded polystyrene foam core. Mohammadimehr and Shahedi [14] investigated the high-order buckling and free vibration behaviors sandwich beams using the generalized differential quadrature method.

This study is carried out on vibroacoustic response of a finite orthotropic laminated composite rectangular plate under a sound wave excitation in thermal environments by analytical method. The plate is assumed to be clamped on all four sides mounted on an infinite acoustic rigid baffle. The sound transmission loss is calculated from the ratio of incident to transmitted acoustic powers. Different influences: the composite materials types, the thermal loads, the incident and azimuth angles on STL are evaluated.

2. THEORETICAL FORMULATION

2.1. Plate geometry and assumption

Consider a finite, rectangular laminated composite plate clamped in an infinite acoustic rigid baffle, as shown in Figs. 1(a) and 1(b). The plate has length a along x-direction,

width b along y-direction and thickness h along z-direction, with $h << a$ and $h << b$ assumed.

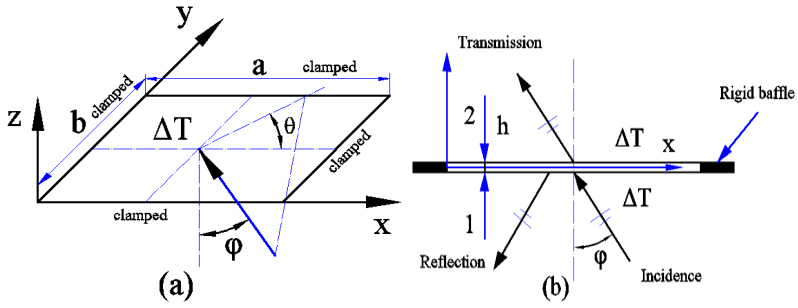

Fig. 1. Schematic of sound transmission through a clamped composite plate: (a) overall vie; (b) view from the direction of arrow in (a)

The plate divides the spatial region into two regimes, i.e., the incident field $(z < 0)$ and the transmitted field $(z > 0)$. An oblique plane sound wave varying harmonically in time is incident on the bottom side of the plate, with elevation angle, φ and azimuth angle, θ, Fig. 1(b). The incident sound wave excites the plate causing the plate to vibrate and divides space into three regions: the incident domain, the reflected domain, and the transmitted domain.

2.2. Composite laminate plate dynamics

The dynamical displacement of an orthotropic symmetric laminated composite plate in the air on both sides and subjected to uniform, plane sound wave varying harmonically can be described by [6]

$$D_{11}\frac{\partial^4 w(x,y;t)}{\partial x^4} + 2(D_{12}+2D_{66})\frac{\partial^4 w(x,y;t)}{\partial x^2\partial y^2} + D_{22}\frac{\partial^4 w(x,y;t)}{\partial y^4} + m^*\frac{\partial^2 w(x,y;t)}{\partial t^2} - \left(N_1\frac{\partial^2 w(x,y;t)}{\partial x^2} + N_2\frac{\partial^2 w(x,y;t)}{\partial y^2}\right) = j\omega\rho_0\left[\Phi_1(x,y,z;t) - \Phi_2(x,y,z;t)\right], \tag{1}$$

where D_{ij} $(ij = 11, 12, 66, 22)$ is the flexural rigidity, m^* is the surface density of the plate, ρ_0 is the air density, ω is the angular frequency of the incident sound and $\Phi_i (i = 1, 2)$ are the velocity potentials for the incidence field and the transmistted field, respectively. N_i $(i = 1, 2)$ are constants determined by

$$N_i = \sum_{k=1}^{N}\int_{z_{k-1}}^{z_k}[Q_{ij}]_k\alpha_j\Delta T\,\mathrm{d}z, \quad (i,j=1,2), \tag{2}$$

where α_j $(j = 1, 2)$ are coefficients of thermal expansion in longitudinal and transverse direction; ΔT is temperature difference (is assumed to be constant in this study).

The flexural rigidity of laminated composite plate is determined by

$$D_{ij} = \frac{1}{3}\sum_{k=1}^{n} Q_{ij}^{k}\left(z_{k+1}^{3} - Z_{k}^{3}\right), \tag{3}$$

where the reduced stiffnesses of the k^{th} layer are defined as

$$Q_{11} = \frac{E_1}{1-\nu_{12}\nu_{21}},\quad Q_{12} = \frac{\nu_{12}E_2}{1-\nu_{12}\nu_{21}},\quad Q_{22} = \frac{E_2}{1-\nu_{12}\nu_{21}},\quad Q_{66} = G_{12},\quad \frac{\nu_{12}}{E_1} = \frac{\nu_{21}}{E_2}, \tag{4}$$

and $E_1, E_2, G_{12}, \nu_{12}$ are the k^{th} layer elastic constants.

Note that, for an isotropic plate, $D_{11} = D_{22} = Eh^3/[12(1-\nu^2)], D_{12} = \nu D_{11}, D_{66} = Gh^3/12$.

The displacement of the composite plate induced by the incident sound can be expressed as

$$w\left(x,y;t\right) = w_0 e^{-j\left(k_x x + k_y y - \omega t\right)}. \tag{5}$$

The acoustic velocity potential in the incidence field (Fig. 1) is defined as [6]

$$\Phi_1\left(x,y,z;t\right) = I_{mn}e^{-j\left(k_x x + k_y y + k_z z - \omega t\right)} + \beta_{mn}e^{-j\left(k_x x + k_y y - k_z z - \omega t\right)}, \tag{6}$$

where I and β are the amplitudes of the incident (positive-going) and the reflected (negative-going) waves, respectively.

Similarly, the velocity potential in the transmitting waves, given as [6]

$$\Phi_2\left(x,y,z;t\right) = \varepsilon_{mn}e^{-j\left(k_x x + k_y y + k_z z - \omega t\right)}, \tag{7}$$

where ε is the amplitude of the radiating (positive-going) wave.

These wave numbers are determined by the elevation angle, φ and azimuth angle, θ of the incident sound wave as

$$k_x = k_0 \sin\varphi\cos\theta,\quad k_y = k_0 \sin\varphi\sin\theta,\quad k_z = k_0\cos\varphi, \tag{8}$$

where $k_0 = \omega/c_0$ is the acoustic wave number in air and c_0 is the acoustic speed in the air.

With the plate fully clamped onto a rigid baffle, the boundary conditions can be expressed as

$$\text{At } x = 0, a;\quad \forall 0 < y < b,\quad w = 0,\quad \frac{\partial w}{\partial x} = 0, \tag{9}$$

$$\text{At } y = 0, b;\quad \forall 0 < x < a,\quad w = 0,\quad \frac{\partial w}{\partial y} = 0. \tag{10}$$

At the air-plate interface the normal velocity is continuous, yielding the corresponding velocity compatibility condition equations

$$\text{At } z = 0,\quad -\frac{\partial \Phi_1}{\partial z} = -\frac{\partial \Phi_2}{\partial z} = j\omega w, \tag{11}$$

$$\text{At } z = h,\quad -\frac{\partial \Phi_1}{\partial z} = -\frac{\partial \Phi_2}{\partial z} = j\omega w. \tag{12}$$

Under the excitation of harmonic sound waves, the transverse deflection of the composite plates can be expressed in a form of modal decomposition

$$w\left(x,y;t\right)=\sum_{m,n=1}^{\infty}\varphi_{mn}\left(x,y\right)q_{mn}(t), \tag{13}$$

where the modal function, φ_{mn} and modal coefficient, q_{mn} are given by

$$\varphi_{mn}\left(x,y\right)=\left(1-\cos\frac{2m\pi x}{a}\right)\left(1-\cos\frac{2n\pi y}{b}\right),\quad q_{mn}\left(t\right)=\alpha_{mn}e^{j\omega t}. \tag{14}$$

Similarly, the acoustical velocity potentials of Eqs. (6) and (7) are expressed as

$$\Phi_1\left(x,y,z;t\right)=\sum_{m,n=1}^{\infty}I_{mn}\varphi_{mn}e^{-j(k_z z-\omega t)}+\sum_{m,n=1}^{\infty}\beta_{mn}\varphi_{mn}e^{-j(-k_z z-\omega t)}, \tag{15}$$

$$\Phi_2\left(x,y,z;t\right)=\sum_{m,n=1}^{\infty}\varepsilon_{mn}\varphi_{mn}e^{-j(k_z z-\omega t)}. \tag{16}$$

Let ξ_1 and ξ_2 represent the acoustic particle displacement in the incident and transmitted air medium, respectively. The air particle displacement and the acoustic pressure are related by the air momentum equation, as

$$\frac{\partial^2}{\partial t^2}\xi_1=-\frac{1}{\rho_0}\frac{\partial p_1}{\partial z}\bigg|_{z=0},\quad \frac{\partial^2}{\partial t^2}\xi_2=-\frac{1}{\rho_0}\frac{\partial p_2}{\partial z}\bigg|_{z=0}, \tag{17}$$

where p_i $(i=1,2)$, the acoustic pressure can be expressed by Bernoull's equation, as

$$p_i=\rho_0\left[\frac{\partial\Phi_i}{\partial t}\right],\quad (i=1,2). \tag{18}$$

The displacements of the air particle adjacent to the plate can be expressed as

$$\xi_1=\xi_{10}e^{-j\left(k_x x+k_y y-\omega t\right)},\quad \xi_2=\xi_{20}e^{-j\left(k_x x+k_y y-\omega t\right)}. \tag{19}$$

Substituting (18)–(19) into (17) and applying the acoustical velocity potentials of (15) and (16), one can obtain

$$\begin{aligned}\xi_{10}&=\left(\sum_{m,n=1}^{\infty}I_{mn}\varphi_{mn}-\sum_{m,n=1}^{\infty}\beta_{mn}\varphi_{mn}\right)\frac{k_z}{\omega}e^{j\left(k_x x+k_y y\right)},\\ \xi_{20}&=\sum_{m,n=1}^{\infty}\varepsilon_{mn}\varphi_{mn}\frac{k_z}{\omega}e^{j\left(k_x x+k_y y\right)}.\end{aligned} \tag{20}$$

The factual case that the composite plate immersed in an air medium requires that the displacements of the air particles adjacent to the panel should be the same as those of the attached panel particles. Accordingly, the displacement continuity condition can be written as

$$\xi_{10}=w_0|_{z=0},\quad \xi_{20}=w_0|_{z=h}. \tag{21}$$

The following relation between coefficients I_{mn} and I_0 is obtained

$$I_{mn} = \frac{4I_0 abk_x^2 k_y^2 \left(1 - e^{-jak_x}\right)\left(1 - e^{-jbk_y}\right)}{\left(4m^2\pi^2 - a^2k_x^2\right)\left(4n^2\pi^2 - b^2k_y^2\right)}. \tag{22}$$

One can express the coefficients in the acoustical velocity potentials by the plate displacement coefficients, as

$$\beta_{mn} = I_{mn} - \frac{\omega}{k_z}\alpha_{mn}, \quad \varepsilon_{mn} = \frac{\omega}{k_z}\alpha_{mn}. \tag{23}$$

Substituting (13)–(14) into (1) and applying the orthogonality of the modal functions, one gets

$$\ddot{q}_{mn} + \omega_{mn}^2 q_{mn}(t) - \frac{j\omega\rho_0}{m^*}\left[\begin{array}{l} I_{mn}e^{-j(k_z z - \omega t)} + \beta_{mn}e^{-j(-k_z z - \omega t)} - \varepsilon_{mn}e^{-j(k_z z - \omega t)} + \\ 4N_1\left(\frac{m\pi}{a}\right)^2 + 4N_2\left(\frac{n\pi}{b}\right)^2 \end{array}\right] = 0, \tag{24}$$

where, $\ddot{q}_{mn}(t)$ is the plate displacement second-order differential, $q_{mn}(t) = \alpha_{mn}e^{j\omega t}$; ω_{mn} is the natural frequencies of the orthotropic cross-ply rectangular laminated composite plate are determined by the plate properties, as

$$\begin{aligned} \omega_{mn}^2 = {} & \frac{\pi^4}{I^* b^4}\left[\frac{48}{9}D_{11}m^4\left(\frac{b}{a}\right)^4 + 2\left(D_{12} + 2D_{66}\right)\frac{16}{9}m^2n^2\left(\frac{b}{a}\right)^2 + \frac{48}{9}D_{22}n^4\right] \\ & + \frac{\pi^2}{I^*}\left[N_1\left(\frac{m}{a}\right)^2 + N_2\left(\frac{n}{b}\right)^2\right], \end{aligned} \tag{25}$$

where $I^* = \sum_{k=1}^{n}\rho_0^{(k)}\left(h_{k+1} - h_k\right)$. Therefore, the modal coefficients, α_{mn} is determined by

$$\alpha_{mn} = \frac{2j\omega\rho_0}{m^*}\left[I_{mn} + 2N_1\left(\frac{m\pi}{a}\right)^2 + 2N_2\left(\frac{n\pi}{b}\right)^2\right]\left[\omega_{mn}^2 - \omega^2 + 2\frac{j\omega^2\rho_0}{m^*k_z}\right]^{-1}. \tag{26}$$

Once the panel displacement coefficients, α_{mn} are known, the acoustical velocity potentials will be known, given by

$$\Phi_1(x,y,0) = 2Ie^{-j\left(k_x x + k_y y\right)} - \frac{\omega}{k_z}\sum_{m,n=1}^{\infty}\alpha_{mn}\varphi_{mn}(x,y), \tag{27}$$

$$\Phi_2(x,y,0) = \frac{\omega}{k_z}\sum_{m,n=1}^{\infty}\alpha_{mn}\varphi_{mn}(x,y). \tag{28}$$

3. DEFINITION OF SOUND TRANSMISSION LOSS

The power of incident sound is defined as [6]

$$\Pi_1 = \frac{1}{2}Re\int_0^b\int_0^a p_1 v_1^* \mathrm{d}x\mathrm{d}y, \tag{29}$$

where, the asterisk symbol denotes complex conjugate, $v_1^* = p_1/(\rho_0 c_0)$ is the local acoustic velocity, and

$$p_1 = j\rho_0\omega\Phi_1(x,y,0) = j\rho_0\omega\left[2I_{mn}e^{-j\left(k_x x+k_y y\right)} - \frac{\omega}{k_z}\sum_{m,n=1}^{\infty}\alpha_{mn}\varphi_{mn}(x,y)\right], \tag{30}$$

is the sound pressure in the incident field. Substitution p_1 and v_1^* into (29) yields

$$\Pi_1 = \frac{\rho_0\omega^2}{2c_0}\left|4I_{mn}^2\int_0^b\int_0^a e^{-2j\left(k_x x+k_y y\right)}\,\mathrm{d}x\mathrm{d}y - 4I_{mn}\frac{\omega}{k_z}\sum_{m,n=1}^{\infty}\alpha_{mn}\int_0^b\int_0^a e^{-j\left(k_x x+k_y y\right)}\varphi_{mn}\mathrm{d}x\mathrm{d}y\right.$$
$$\left.+\frac{\omega^2}{k_z^2}\sum_{m,n=1}^{\infty}\sum_{k,l=1}^{\infty}\alpha_{mn}\alpha_{kl}\int_0^b\int_0^a\varphi_{mn}(x,y)\,\varphi_{kl}(x,y)\,\mathrm{d}x\mathrm{d}y\right|. \tag{31}$$

The transmitted sound power can be defined as [6]

$$\Pi_2 = \frac{1}{2}Re\int_0^b\int_0^a p_2 v_2^*\mathrm{d}x\mathrm{d}y, \tag{32}$$

where, $v_2^* = p_2/(\rho_0 c_0)$ is the local acoustic velocity and

$$p_2 = j\rho_0\omega\Phi_2(x,y,0) = j\rho_0\frac{\omega^2}{k_z}\sum_{m,n=1}^{\infty}\alpha_{mn}\varphi_{mn}(x,y), \tag{33}$$

is the sound pressure in the transmitted field. Combination of Eqs. (32) and (33) and the expression of v_2^* results in

$$\Pi_2 = \frac{\rho_0\omega^4}{2c_0k_z^2}\left|\sum_{m,n=1}^{\infty}\sum_{k,l=1}^{\infty}\alpha_{mn}\alpha_{kl}\int_0^b\int_0^a\varphi_{mn}(x,y)\,\varphi_{kl}(x,y)\mathrm{d}x\mathrm{d}y\right|. \tag{34}$$

The power transmission coefficient can be obtained as [6]

$$\tau_0(\theta,\varphi,f) = \frac{\Pi_2}{\Pi_1}. \tag{35}$$

Then the sound transmission loss across the composite plate is defined by [6]

$$STL = 10\log_{10}\left(\frac{1}{\tau_0(\varphi,\theta,f)}\right). \tag{36}$$

4. VALIDATIO

For validation, the theoretical STL is compared with the experimental results of Kuo [5] through two typical orthotropic laminated composite plates: $[UD]_7$ and $[Rovin]_7$

are excited by wave varying harmonically with incident angle, $\varphi = 30^\circ$ and azimuth angle, $\theta = 30^\circ$ and $\Delta T = 0^\circ$C. Each of two plates comprises seven layers of glass fiber composite. Exactly, the laminating sequence of $[UD]_7$ is $[0^0/0^0/0^0/0^0/0^0/0^0/0^0]$ and [rovin/rovin/rovin/rovin/rovin/rovin/rovin] for $[Rovin]_7$. Note that the composite material $[UD]_7$ is a transverse isotropic materia; $[Rovin]_7$ is an orthotropic material. The finite-size plate is 120 cm $\times$ 120 cm. Table 1 presents the mechanical properties of the materials used for the plates. The property parameters of plates is presented in Table 1. Speed of sound in air, $c = 343$ m/s; the density of the air, $\rho_0 = 1.21$ kg/m^3 and the initial amplitude, $I_0 = 1$ m^2/s.

Table 1. Mechanical properties of composite materials

Material	E_{11} (GPa)	E_{22} (GPa)	E_{33} (GPa)	G_{12} (GPa)	G_{13} (GPa)	G_{23} (GPa)	υ_{12}	υ_{13}	υ_{23}	Thickness (mm)	Density (kg/m^3)
UD	37.8	13.1	13.1	8	8	5.3	0.25	0.25	0.25	0.503	1633
Rovin	24	24	10.5	9	8	8	0.25	0.25	0.25	0.429	1531

We see a good agreement between the comparison results for all two types of composite plates. The difference between the current sound transmission loss values and the experimental results of Kuo [5] for all two layered composite plates is less than 5 dB over the entire 1/3 Octave frequency range.

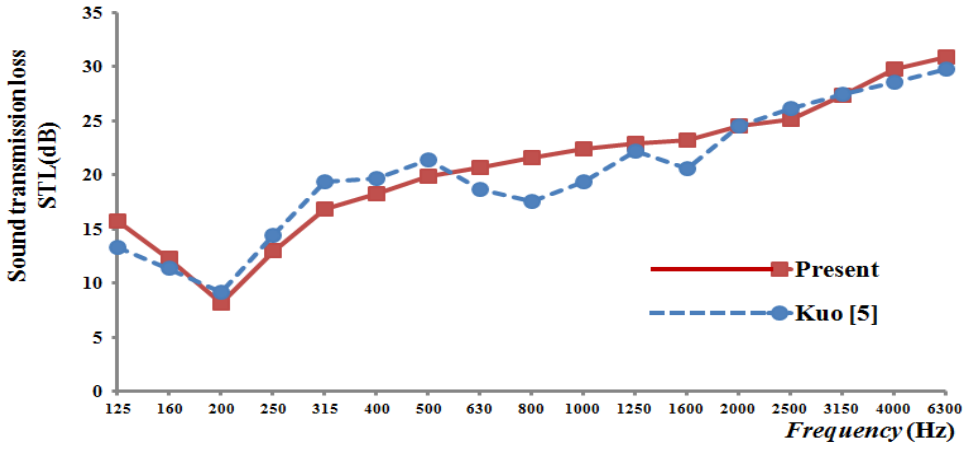

Fig. 2. Comparison STL between present numerical calculation and experimental results of Kuo [5] through $[UD]_7$ plate

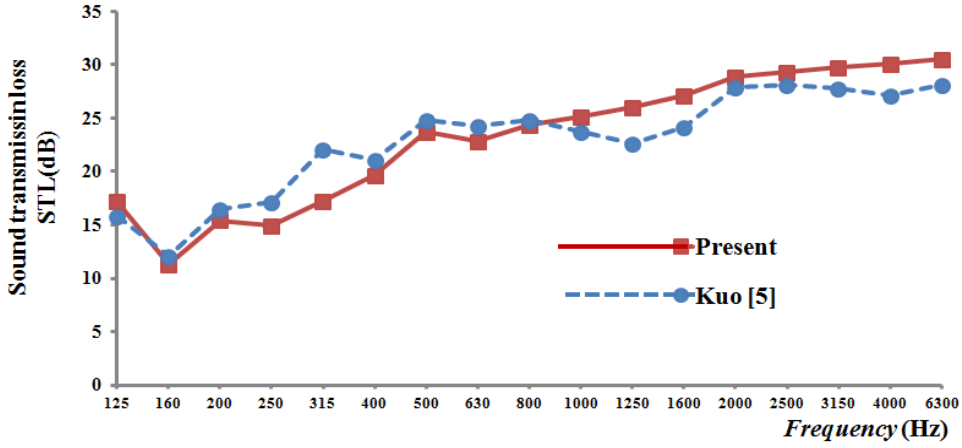

Fig. 3. Comparison STL between present numerical calculation and experimental results of Kuo [5] through $[\text{Rovin}]_7$ plate

5. NUMERICAL RESULTS AND DISCUSSION

5.1. Influence of composite materials type on STL

The influence of composite materials on STL through a finite clamped laminated composite plates is studied in this section by selecting three types of composite materials: Fiberglass/Epoxy, Graphite/Epoxy and Kevlar/Epoxy are excited by wave varying harmonically with incident angle, $\varphi = 30^\circ$ and azimuth angle, $\theta = 30^\circ$ under thermal loads $\Delta T = 0^\circ$C and $\Delta T = 20^\circ$C The composite plates are composed of 8 balanced, symmetrical layers, with a configuration of $[0/90/0/90]_s$. The mechanical properties of composite material are shown in Table 2. Speed of sound in air, c = 343 m/s; the density of the air, ρ_0 = 1.21 kg/m^3 and the initial amplitude, I_0 = 1 m^2/s. The results are shown in Fig. 4.

Table 2. Composite materials properties and the geometrical dimensions

Composite	E_1 (GPa)	E_2 (GPa)	G_{12} (GPa)	ν_{12}	ρ (kg/m^3)	a (m)	b (m)	h (mm)
Kevlar/epoxy	76	6	2	0.34	1360	0.91	1.52	1.02
Graphite/epoxy	137	10	5	0.30	1550	0.91	1.52	1.02
Fiberglass/epoxy	39	9	2	0.30	2190	0.91	1.52	1.02

From Figs. 4(a) and 4(b), it can be seen that, under the effect of thermal load, the STL curve changes significantly, especially in the frequency region, $f < 800$ Hz. The occurrence of dip points is more because the thermal environment is a cruel factor that results in thermal stresses internal to the structures, modifies the stiffness of the structural system, and alters the dynamic characteristics of the system essentially. Leads to a significant drop in the STL value when the plate is in a thermal environment especially in the high frequency region, $f > 900$ Hz. Therefore, plates in a thermal environments have less sound insulation than in a non-thermal environments.

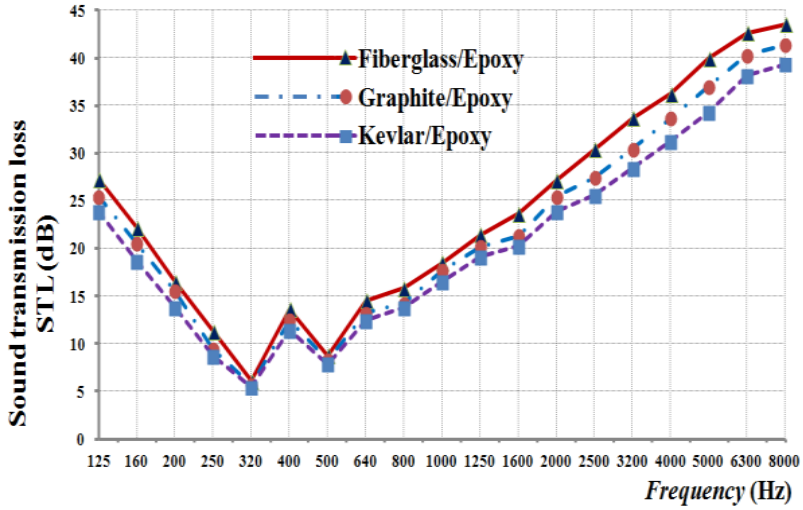

(a) Thermal load, $\Delta T = 0^{\circ}$C

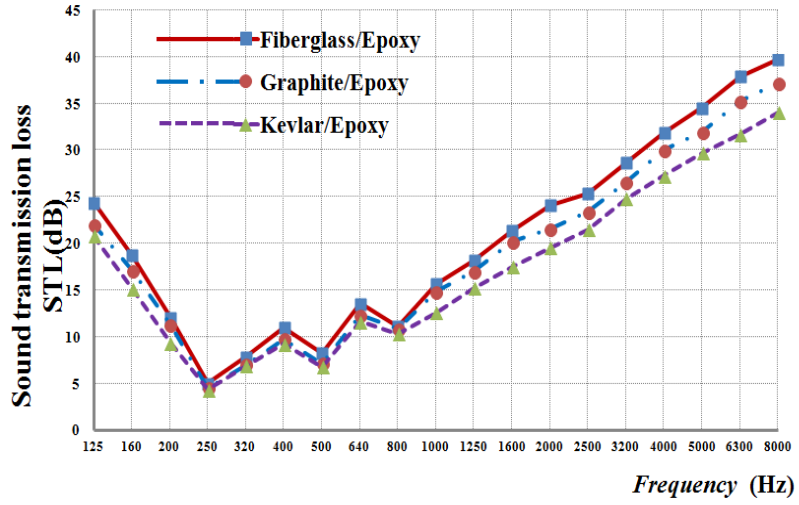

(b) Thermal load, $\Delta T = 20^{\circ}$C

Fig. 4. Influence of composite materials on STL of a clamped composite plate

5.2. Influence of the thermal load on STL

In order to quantify the effects of the temperature on STL through the Fiberglass/epoxy laminated composite plate excited by wave varying harmonically with incident angle, $\varphi = 30^{\circ}$ and azimuth angle, $\theta = 30^{\circ}$, in this section, four temperature load, $\Delta T = 0^{\circ}$C, 20°C, 30°C and 40°C are imposed on the composite plate. The geometrical and material parameters are shown in the Table 2. Speed of sound in air, $c = 343$ m/s; the density of the air, $\rho_0 = 1.21$ kg/m^3 and the initial amplitude, $I_0 = 1$ m^2/s.

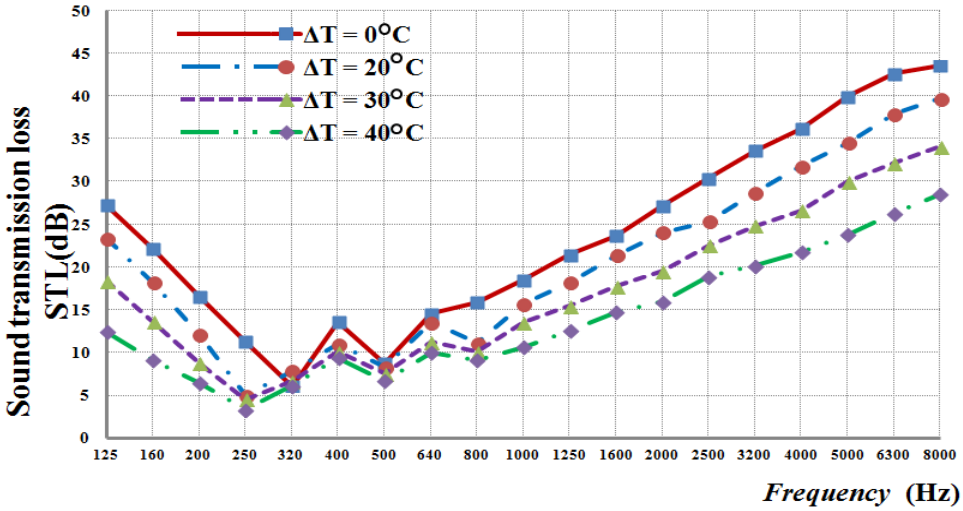

Fig. 5. Influence of the temperature load on STL

The Fig. 5 depicts the curves of STL in different temperature load, ΔT. It manifests that the peaks and the dips tend to decrease and flow to the lower frequencies with the increment of the temperature load. The reason is, obviously, that temperature softens the stiffness of the structure and decreases the natural frequencies due to the internal compressive stresses. As can be observed, for this reason, the STL decreases as the temperature load rises especially in the low frequency range.

5.3. Influence of the incident angle on ST

The influence of sound incident angles (elevation angle and azimuth angle) on STL through the Graphite/epoxy laminated composite plate excited by wave varying harmonically under temperature load, $\Delta T = 20^{\circ}$C. We consider two cases of influence of incident angle on STL as follows: change of elevatio angle, $\varphi = 0^{\circ}, 30^{\circ}, 45^{\circ}, 60^{\circ}$ and azimuth angle fixed at $\theta = 30^{\circ}$; change of azimuth angle, $\theta = 0^{\circ}, 30^{\circ}, 45^{\circ}, 60^{\circ}$ and elevation angle fixed at $\varphi = 30^{\circ}$. The geometrical and material parameters are shown in the Tab.2. Speed of sound in air, $c = 343$ m/s; the density of the air, $\rho_0 = 1.21$ kg/m^3 and the initial amplitude, $I_0 = 1$ m^2/s. The results are shown in Fig. 6 and Fig. 7.

From Fig. 6 obviously, the STL decreases with the increment of the incident angle. Consequently, a smaller incident angle of sound results in a promising capability of sound insulation. Fig. 7 shows that, azimut angles slightly impact on the STL. But in the high frequency range, the STL is slightlydifferent along with various azimuth angles due to the anisotropy of the plate.

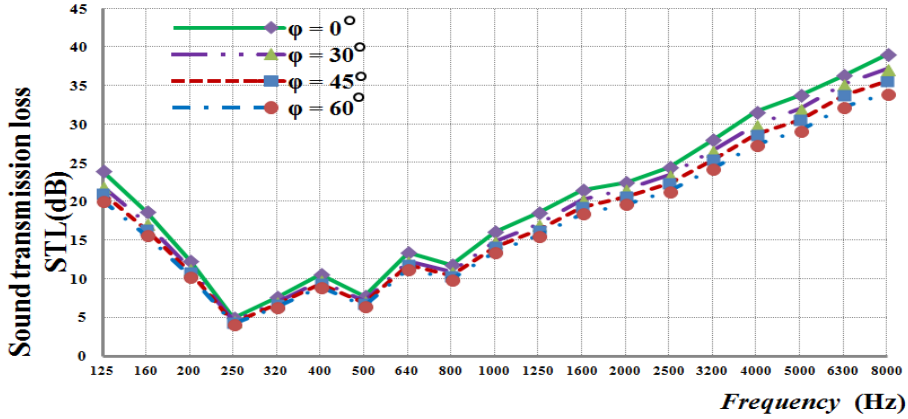

Fig. 6. IInfluence of the elevation angle on STL, $\theta = 30^\circ$

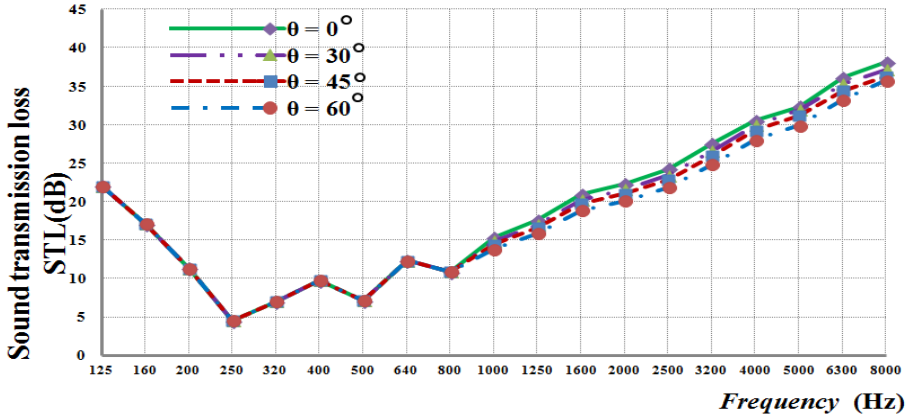

Fig. 7. Influence of the azimuth angle on STL, $\varphi = 30^\circ$

6. CONCLUSIONS

An analytical approach has been developed to study the vibroacoustic behavior and the sound transmission loss across a finite clamped orthotropic laminated composite under a sound wave excitation in thermal environments. We get some of the following conclusions:

- The theoretical predictions on STL are in good agreement with existing results.
- The plates in a thermal environment have less sound insulation than in a non-thermal environment.
- The temperature softens the stiffness of the structure and decreases the natural frequencies due to the internal compressive stresses. Therefore, the STL of the clamped composite plates decreases as the temperature load rises especially in the low frequency range.

- The incident angle has a stronger influence than the azimuth angle on the sound transmission loss.

DECLARATION OF COMPETING INTEREST

The authors declare that they have no known competing financial interests or personal relationships that could have appeared to influence the work reported in this paper.

FUNDING

This research received no specific grant from any funding agency in the public, commercial, or not-for-profit sectors.

REFERENCES

[1] S. H. Ko. Reduction of structure-borne noise using an air-voided elastomer. *The Journal of the Acoustical Society of America*, **101**, (1997), pp. 3306–3312. https://doi.org/10.1121/1.418292.

[2] A. Tadeu and J. Antonio. Acoustic insulation of single panel walls provided by analytical expressions versus the mass law. *Journal of Sound and Vibration*, **257**, (2002), pp. 457–475. https://doi.org/10.1006/jsvi.2002.5048.

[3] A. Tadeu, J. Antonio, and N. Simoes. Acoustic insertion loss provided by single and double steel panels separating an air from a water medium. *Acta Acoustica/Acustica*, **89**, (3), (2003), pp. 391–405.

[4] H.-J. Lin, C.-N. Wang, and Y.-M. Kuo. Sound transmission loss across specially orthotropic laminates. *Applied Acoustics*, **68**, (2007), pp. 1177–1191. https://doi.org/10.1016/j.apacoust.2006.06.007.

[5] Y.-M. Kuo, H.-J. Lin, and C.-N. Wang. Sound transmission across orthotropic laminates with a 3D model. *Applied Acoustics*, **69**, (2008), pp. 951–959. https://doi.org/10.1016/j.apacoust.2007.08.002.

[6] T. I. Thinh and P. N. Thanh. Vibroacoustic response of a finite clamped laminated composite plate. In *Advances in Engineering Research and Application*, pp. 589–600. Springer International Publishing, (2018). https://doi.org/10.1007/978-3-030-04792-4_76.

[7] B. Pan, D. Wu, and Y. Xia. High-temperature deformation field measurement by combining transient aerodynamic heating simulation system and reliability-guided digital image correlation. *Optics and Lasers in Engineering*, **48**, (2010), pp. 841–848. https://doi.org/10.1016/j.optlaseng.2010.04.007.

[8] B. Budiansky and J. Mayers. Influence of aerodynamic heating on the effective torsional stiffness of thin wings. *Journal of the Aeronautical Sciences*, **23**, (1956), pp. 1081–1093. https://doi.org/10.2514/8.3735.

[9] H. V. Tung. Nonlinear thermomechanical response of pressure-loaded doubly curved functionally graded material sandwich panels in thermal environments including tangential edge constraints. *Journal of Sandwich Structures & Materials*, **20**, (2017), pp. 974–1008. https://doi.org/10.1177/1099636216684312.

[10] Y. Frostig. Classical and high-order computational models in the analysis of modern sandwich panels. *Composites Part B: Engineering*, **34**, (2003), pp. 83–100. https://doi.org/10.1016/s1359-8368(02)00073-2.

[11] Z. Sun, S. Shi, X. Guo, X. Hu, and H. Chen. On compressive properties of composite sandwich structures with grid reinforced honeycomb core. *Composites Part B: Engineering*, **94**, (2016), pp. 245–252. https://doi.org/10.1016/j.compositesb.2016.03.054.

[12] Z. Wang, J. Liu, Z. Lu, and D. Hui. Mechanical behavior of composited structure filled with tandem honeycombs. *Composites Part B: Engineering*, **114**, (2017), pp. 128–138. https://doi.org/10.1016/j.compositesb.2017.01.018.

[13] U. Caliskan and M. K. Apalak. Low velocity bending impact behavior of foam core sandwich beams: Experimental. *Composites Part B: Engineering*, **112**, (2017), pp. 158–175. https://doi.org/10.1016/j.compositesb.2016.12.038.

[14] M. Mohammadimehr and S. Shahedi. High-order buckling and free vibration analysis of two types sandwich beam including AL or PVC-foam flexible core and CNTs reinforced nanocomposite face sheets using GDQM. *Composites Part B: Engineering*, **108**, (2017), pp. 91–107. https://doi.org/10.1016/j.compositesb.2016.09.040.